

Dual-Scheduler Design for C/U-plane Decoupled Railway Wireless Networks

Li Yan, *Student Member, IEEE*, Xuming Fang, *Member, IEEE*, Yuguang Fang, *Fellow, IEEE*, and Xiangle Cheng

Abstract—Previously, we have proposed a C/U-plane (Control/User plane) decoupled railway wireless network in which higher frequency bands are adopted by small cells to provide wider available spectra for the U-plane of passengers' services. In order to guarantee reliable connectivity to wayside eNodeBs (eNBs), an onboard mobile relay (MR), consisting of two components, namely, MR-UE (User Equipment) and MR-AP (Access Point), is employed to forward passengers' services over backhaul links between MR-UE and wayside eNBs. The remaining problem here is how to utilize spectra effectively and efficiently under this new configuration. Since a given wayside eNB hosts only one single accessed user most of the time, we design an additional uplink scheduler for the MR-UE to self-manage the usage of uplink resources, avoiding the complicated uplink grant procedure commonly used in the conventional cellular systems. Moreover, we develop eNB schedulers to coordinate the spectra in small cells. To deal with occasional multi-user scenarios, we propose an uplink scheduler switcher for the macro cell to judge which uplink scheduler should be activated. Furthermore, an uplink resource allocation scheme with high spectrum efficiency is deliberately designed for the new dual-scheduler configuration. Finally, we carry out theoretical analysis and numerical simulations to demonstrate the effectiveness of our proposed scheme.

Index Terms—Scheduling, resource allocation, railway systems, C/U-plane decoupled architecture.

I. INTRODUCTION

WITH remarkable progress in railway industry and mobile Internet, train passengers, especially those in long-distance journeys, may demand good Internet access onboard. However, the limited capacity of existing narrow-band railway wireless communication systems makes this a significant challenge. To meet these new capacity demands, railway wireless communication systems are confronting with the evolution to the next generation. With enhanced data rate, LTE (Long Term Evolution) networks are viewed as a potential candidate for this evolution [1], [2]. Nevertheless, with the increasingly growing wireless service demands of onboard passengers and advanced security monitoring devices in trains, we still need to study new network architecture and advanced technologies that are suitable for railways to meet these forthcoming demands. In the following subsections, we first introduce

L. Yan, and X. Fang are with Key Lab of Info Coding & Transmission, Southwest Jiaotong University, Chengdu 610031, China. (E-mails: Liyan12047001@my.swjtu.edu.cn; xmfang@swjtu.edu.cn).

Y. Fang is with the Department of Electrical and Computer Engineering, University of Florida, PO Box 116130, Gainesville, FL 32611 (E-mail: fang@ece.ufl.edu).

X. Cheng is with the Department of Mathematics and Computer Science, College of Engineering, Mathematics and Physical Sciences, University of Exeter, Exeter, EX4 4QF, U.K (E-mail: leabc.love@163.com).

the development of railway wireless communication systems and present C/U-plane decoupled railway wireless networks. Then, we discuss the problems in uplink scheduling under almost single-user railway scenarios. Finally, we propose dual-scheduler solutions to solve these problems.

A. State-of-the-Art

To deal with the exponentially increasing traffic in public mobile networks, higher frequency bands with wider available spectra, including frequency bands from 5GHz to 300GHz, are being considered in upcoming 5G (Generation) wireless communication systems [3], [4]. However, the large propagation loss of higher frequency bands limits the signal coverage. Smaller coverage means more handovers, from which the subsequently redundant control signaling aggravates the network burden. Fortunately, C/U-plane decoupled architecture proposed in [5], [6] presents a potential solution. In our previous work [7], [8], we have started this research on application of C/U-plane decoupled architecture to railway wireless communication systems. The detailed C/U-plane decoupled architecture is depicted in Fig. 1. Considering the investment return, no public mobile network operator would offer full coverage for most sparsely-populated railway scenarios. Moreover, on account of the severe challenges faced by the railway scenarios like high penetration loss and frequent group handover, it is difficult for user equipments to hold a reliable direct connection with wayside eNBs. Hence, as shown in Fig. 1, onboard mobile relay is employed on the top of a train to forward passengers' services. Generally, MR has dual attributes, i.e., it communicates as either an eNB/access point with UEs or an UE with an eNB. For clarity, function specific modules MR-UE and MR-AP, which are connected to each other via optical fibers, are separately mounted on the roofs inside and outside the train. Passengers' services are firstly collected by MR-AP and then forwarded to wayside eNBs via MR-UE. Usually, the link between an internal passenger and an MR-AP is called access link. While the link between an MR-UE and a wayside eNB is called backhaul link [9]. To simplify the analysis, we assume that out-band mobile relay is applied. In C/U-plane decoupled railway wireless networks, the wider available spectra of small cells are assigned to backhaul links. In this paper, we focus on the spectrum utilization of backhaul links, so that the whole train can be regarded as one user, i.e., onboard MR-UE.

B. Problems in Uplink Scheduling

As a matter of fact, there exist many differences between the railway and public mobile scenarios, among which the most

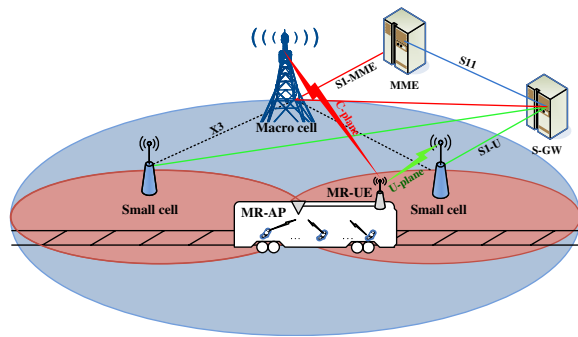


Fig. 1. The C/U-plane decoupled railway wireless network.

prominent one is the number of accessed users. Traditionally, multiple users simultaneously access to a given eNB in public mobile networks and these users have no knowledge about other users, such as the channel state information (CSI), resource usages and even the existence of others. Hence, in multi-user public mobile networks, the uplink and downlink schedulers are both configured in eNBs to harmonize the spectrum sharing among these users in a centralized fashion.

For downlink, all served users feed back their downlink CSIs and service requirements to eNBs. Then based on these feedbacks, eNBs make their decisions about what and how many RBs (Resource Blocks) are assigned to each user and which MCS (Modulation and Coding Scheme) is used in these RBs. Meanwhile, the resource allocation results carried by PDCCH (Physical Downlink Control Channel) are sent to users to help them decode downlink data. In LTE networks, to reduce the overhead on PDCCH all RBs assigned to one user employ the same MCS [10], [11]. For uplink, CSIs are directly obtained by eNB through the detection of uplink SRS (Sounding Reference Signal) sent by users. If users have data to transmit, they will send the scheduling request (SR) on PUCCH (Physical Uplink Control Channel). Upon receiving the uplink grant message, the buffer state report (BSR), which contains information about the amount and priority of the following data to send, is transmitted to eNBs on the allocated PUSCH (Physical Uplink Shared Channel). Based on BSR, eNBs determine the resource allocation for the following data. Then the resource allocation carried by PDCCH are sent to users, based on which users transmit the uplink data. Obviously, compared with downlink scheduling procedure, the uplink scheduling procedure suffers longer time delay. Besides, unlike downlink, eNBs cannot exactly track the service requirements of uplink, which heavily degrades the uplink scheduling effectiveness. However, this is inevitable for multi-user public mobile networks.

C. Dual-scheduler Solutions

Despite a few multi-user cases including opposite directional moving trains crossing and station stopping, an onboard MR-UE is almost the single accessed user for a given wayside eNB in railway scenarios. In other words, for a given wayside eNB, the whole spectrum is basically allocated to the single accessed onboard MR-UE. Hence, the problem on how to share the spectrum among multiple users is nonexistent in this

scenario. The conventional eNB-centralized scheduler configuration designed for general mobile systems will unnecessarily decrease its flexibility and increase its delay during the uplink scheduling procedure for most single-user railway scenarios.

In light of the above observation, in the proposed dual-scheduler configuration, we introduce an additional uplink scheduler at the MR-UE. Thus, the MR-UE is able to effectively and flexibly self-manage the resource usage over uplink. According to the characteristics of the C/U-plane decoupled architecture, the eNB schedulers are proposed to be deployed in small cells. In the C/U-plane decoupled architecture, macro cells are the first aware of initial random access requests from other users [6]. In view of practical multi-user railway scenarios, a scheduler switcher is proposed in macro cells. If the onboard MR-UE is the only accessed user, wireless downlink control signaling will be sent by the macro cell to activate the uplink scheduler in the MR-UE. Otherwise, once any other random access request is accepted, control signaling via X3 will be sent from the macro cell towards small cells to select the uplink scheduler in small cells. Meanwhile, wireless downlink control signaling from the macro cell will be transmitted to the MR-UE to terminate its uplink scheduler and inform it to comply with the uplink scheduling from small cells in the subsequent frame.

Under the aforementioned dual-scheduler configuration, an uplink resource allocation scheme with high spectrum efficiency is then proposed to maximize the average throughput under the constraints of BER (Bit Error Rate) requirements and total transmit power. There are a few good reasons behind our design. First, in LTE networks, the resource allocation granularity is RB corresponding to twelve subcarriers in the frequency domain. In railway scenarios where most communications are carried out over viaducts, the wireless channel can be approximately considered as LOS (Line of Sight) with wider coherence bandwidth [1]. Therefore, in the proposed uplink resource allocation scheme, finer resource allocation granularity (e.g., chunk) is employed to reduce the complexity and feedback overhead [12], [13], [14]. Second, according to [11], due to the fact that a large number of RBs within a frame are assigned to one user is infrequent for multi-user scenarios, it will not significantly decrease the spectrum efficiency to allocate the same MCS for all RBs assigned to one user. Hence, as aforementioned, in LTE networks, all services of a user are allocated with the same MCS. However, in most single-user railway scenarios, the whole spectrum of a given wayside eNB is basically allocated to the single accessed onboard MR-UE. It will badly impact the spectrum efficiency to allocate the same MCS for the whole spectrum used by the single MR-UE. Besides, different types of services with various requirements collected from train passengers are all gathered in the onboard MR-UE. Hence, to further improve the spectrum efficiency, different services with various BER requirements are distinguished in the proposed uplink resource allocation scheme. Third, in [15] the similar approach has also been observed. In the proposed resource allocation scheme, various services with different BER requirements are distinguished so as to minimize the total transmit power. While compared with ordinary user equipments, capacity instead of

energy is the main bottleneck for railway wireless networks. Thus, in our proposed uplink resource allocation scheme, the optimization goal is to maximize the average throughput. Finally, most resource allocation schemes to maximize average throughput are based on multi-user scenarios where users have different large-scale SNRs (Signal to Noise Ratios) on the same channel. Thus, it may be better to assign the channel to the user with highest SNR [12][14]. While in the single-user railway scenario, the whole spectrum represents the same large-scale SNR for the onboard MR-UE. Nevertheless, different channels have different instantaneous small-scale fading. Hence, as in [15], [16], our proposed uplink resource allocation scheme is based on the small-scale fading.

The rest of this paper is organized as follows. Section II details the C/U-plane decoupled railway network and the proposed dual-scheduler configuration. In Section III, the uplink resource allocation scheme with high spectrum efficiency is presented. The numerical results are analyzed in Section IV. Finally, Section V concludes this paper.

II. SYSTEM ARCHITECTURE

A. The C/U-plane Decoupled Railway Wireless Network

In LTE networks, one of the most important design principles is to split design space into C-plane and U-plane between MME (Mobility Management Entity) and gateway functionally. The user dedicated data are transmitted on the U-plane from or to SGW (Serving Gateway), while the control signaling designed for network access provisioning is transmitted on the C-plane from or to MME. Based on this observation, in the proposed C/U-plane decoupled architecture for railway wireless networks as shown in Fig. 1, to enable reliable transmission and efficient mobility support, the relatively important C-plane of passengers' services is kept in macro cells using high-quality lower frequency bands. Consequently, control channels such as PDCCH, PUCCH and control signaling related to random access, handover and so on are provided by macro cells. In this way, within a macro cell, the C-plane is always connected and the complicated handover procedures are avoided. As for the major capacity demander, the U-plane of passengers' services is moved to small cells operating at higher frequency bands to gain broader spectra. Correspondingly, PUSCH and PDSCH (Physical Downlink Shared Channel) are moved to small cells. It is notable that small cells have no control functionality, thereby being only connected to SGW as shown in Fig. 1. User data can be directly forwarded to small cells from SGW. Through the X3 interface, small cells are controlled by macro cells that are connected to MME. In addition to the C-plane of passengers' services, some other crucial low-rate services, which have stringent requirements for transmission reliability such as train control information, can also be distributed to macro cells for transmission. Therefore, as shown in Fig. 1, macro cells are connected to SGW as well. More details about the C/U-plane decoupled railway wireless network can be found in [7], [8].

As aforementioned, passengers' equipments inside a train directly connect to the MR-AP and then their data are forwarded to wayside eNBs via MR-UE. In this paper, to simplify

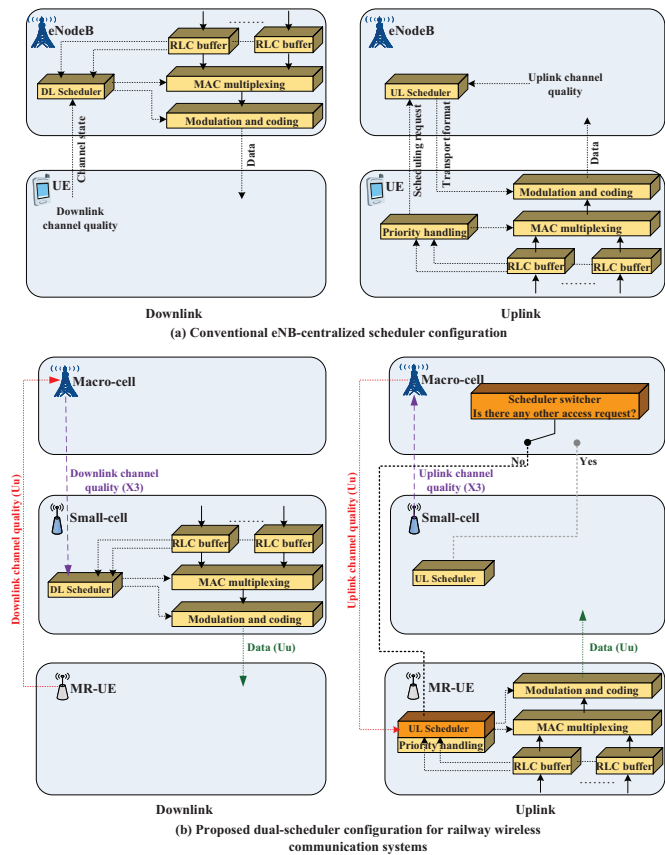


Fig. 2. Scheduler configurations.

the analysis, we only consider one single MR-UE to link the train to wayside eNBs (connecting to the backbone network), and then the whole train is considered as one user. According to [9], backhaul links between MR-UE and wayside eNBs are the key capacity bottlenecks, and should be targeted at operating with high spectrum efficiency. Hence, to meet the capacity demands, the C/U-plane decoupled architecture is employed on backhaul links. In this paper, we focus on the U-plane scheduling of passengers' services to enhance the U-plane spectrum efficiency in backhaul links.

B. The Conventional eNB-centralized Scheduler Configuration

To facilitate the presentation, we take LTE as the baseline for our study. In multi-user public mobile scenarios, uplink and downlink schedulers are both configured in eNBs as shown in Fig. 2(a). We call it eNB-centralized scheduler configuration. In this configuration, users have no control functionality but just feed back some information to help eNBs make the resource allocation decision [10]. As shown in Fig. 2(a), for downlink, an UE feeds back the estimated downlink CSI to the eNB. Then, based on these feedbacks from all served UEs, the eNB makes the resource allocation decision on what and how many RBs and which MCSs are allocated to UEs. Simultaneously, resource allocation decisions are sent over PDCCH to UEs to help them decode respective data on PDSCH. The detailed downlink scheduling procedure is depicted in Fig. 3(a).

In the conventional eNB-centralized scheduler configuration, the uplink scheduler is also arranged in the eNB. The corresponding uplink scheduling procedure is described in Fig. 3(c). The uplink CSIs are directly detected by the eNB through SRS sent by UEs. Once there are uplink data to transmit, the UE will firstly send SR over PUCCH and wait for the response from the eNB. The waiting time T_1 depends on the processing capability and the current traffic load at the eNB. Upon receiving the uplink grant message, BSR and data are transmitted to the eNB after T_2 . For FDD (Frequency Division Duplex) systems, the time delay T_2 is equal to 4ms [10]. While for TDD (Time Division Duplex) systems, the exact value of T_2 depends on the uplink and downlink subframe configuration. Nevertheless, it is not shorter than 4ms. BSR, which consists of the amount and LCG (Logical Channel Group) priority of the subsequent major data to transmit, is the primary reference for the eNB to determine the resource allocation. In LTE networks, to reduce the feedback overhead due to BSR, all logical channels are classified into 4 LCGs. For the eNB, this obviously reduces the tracking accuracy of UE's service requirements, thereby impacting the effectiveness of resource allocation. With BSR, the eNB determines how UEs transmit the following uplink data. Like T_1 , the scheduling time T_3 depends on the processing capability and the current traffic load at the eNB. Upon receiving the uplink grant on PDCCH Format 0, the major data are sent to the eNB after T_4 . The value of T_4 is similar to T_2 . At this time, if a service with higher LCG priority unfortunately arrives, the above obtained resources will be used to transmit that service instead of the previous one that has been allocated with these resources (preemptive scheduling is used here). To some extent, this will decrease the spectrum efficiency. In summary, compared with downlink scheduling procedure, the conventional eNB-centralized uplink scheduling procedure suffers longer delay and less flexibility. However, for multi-user scenarios, this is inevitable.

C. Our Proposed Dual-Scheduler Configuration

Except for occasional multi-user cases (e.g., opposite directional moving trains crossing and station stopping), the onboard MR-UE is almost the single accessed user for a given wayside eNB in railway scenarios. Therefore, how to share the spectrum among multiple users is no longer a problem for this single-user railway scenario. Consequently, a complete adoption of the conventional eNB-centralized scheduler configuration in multi-user scenarios will degrade the performance of the single-user railway scenario. Based on this observation, we propose to add an uplink scheduler at MR-UE, namely, dual-scheduler configuration, as shown in Fig. 2(b) (the function of the new scheduler switcher in macro cells will be illustrated later). Subsequently, in the single-user railway scenario, MR-UE is able to self-manage the usage of uplink resource. For uplink, since MR-UE knows exactly what to transmit, the proposed dual-scheduler configuration improves the effectiveness and flexibility of the uplink scheduling. Furthermore, without the complicated request procedure of uplink grant, significant time is saved. For the eNB scheduler

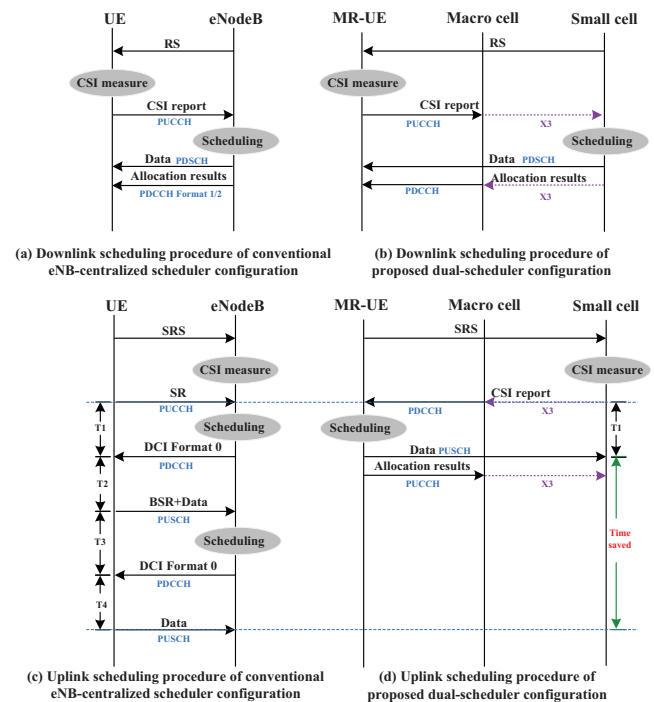


Fig. 3. Scheduling procedures.

configuration, there are two feasible arrangements, that is, for macro cells or small cells. In the C/U-plane decoupled architecture, the U-plane for passengers' services is directly transferred from SGW to small cells, that is, small cells know what to transmit. While as mentioned before, macro cells are connected to SGW to transmit some other possible crucial services, but not the U-plane for passengers' services. Therefore, as shown in Fig. 2(b), to reduce the signaling between small and macro cells, it is more reasonable to set the downlink schedulers in small cells. Nevertheless, as mentioned before, the control signaling related to uplink and downlink scheduling procedures is transferred by macro cells. The signaling between macro and small cells is transmitted via X3. As X3 usually uses optical fibers with extremely wide bandwidth, the time consumption of signaling transfer via X3 is negligible.

Correspondingly, the downlink and uplink scheduling procedures of the proposed dual-scheduler configuration are designed as shown in Fig. 3(b) and Fig. 3(d), respectively. Compared with Fig. 3(a), the downlink scheduling procedure is almost the same, except that all scheduling-related C-plane signaling is transferred by the macro cell via X3. Firstly, the MR-UE sends the estimated downlink CSI of the small cell to the macro cell over PUCCH. Then, this CSI is forwarded to the small cell via X3 to help the downlink scheduler in the small cell make resource allocation decision. After that, the small cell directly sends the downlink data to the MR-UE over PDSCH. Meanwhile, the resource allocation results are transmitted to the macro cell via X3 and then to the MR-UE via the air interface of the macro cell. Since the time consumption over X3 is negligible, no extra delay is brought in. From Fig. 3(d), we can find that the compli-

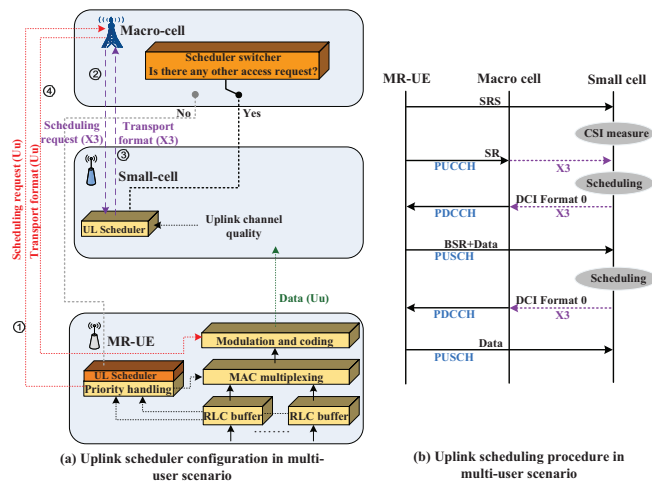


Fig. 4. The proposed dual-scheduler configuration and scheduling procedure for multi-user railway scenarios.

cated uplink grant request process is avoided. Accordingly, the proposed dual-scheduler configuration tremendously saves the uplink scheduling time. Different from the conventional eNB-centralized uplink scheduling procedure, the uplink CSI estimated by the small cell needs to be sent to the macro cell via X3 and then to the MR-UE via the air interface of the macro cell. After the uplink scheduling in the MR-UE, the uplink data and the corresponding resource allocation results are transmitted to the small cell. Similarly, the resource allocation results are then transferred by the macro cell. It is clearly shown that the entire uplink scheduling procedure is just the mirroring process of downlink scheduling procedure in Fig. 3(b).

Considering the occasional multi-user cases in practical railway scenarios, an uplink scheduler is also deployed in the small cell as shown in Fig. 2(b). In the C/U-plane decoupled architecture, initial random access requests are firstly received by macro cells. That is, the macro cell is the first one aware of the existence of any other users. Therefore, a scheduler switcher is introduced into the macro cell to determine which uplink scheduler should be activated based on the condition that whether there are any other random access requests. If the MR-UE is the single accessed user, then the macro cell will send wireless downlink control signaling to activate the uplink scheduler of the MR-UE. Otherwise, the uplink scheduler of the small cell is selected by the signaling from the macro cell via X3. At any time, only one uplink scheduler is activated and the other one acts as a transparent component. While for downlink, the scheduler configuration and scheduling procedure are similar for both multi-user and single-user scenarios. For clarity, the uplink scheduler configuration and scheduling procedure of multi-user scenarios are illustrated in Fig. 4(a) and Fig. 4(b), respectively. From Fig. 4(b), we can find that the uplink scheduling procedure is almost the same as that of the conventional eNB-centralized uplink scheduling procedure, except that all scheduling-related C-plane signaling is transferred by the macro cell.

D. The Corresponding PDCCH and PUCCH Design

Similarly, LTE is taken as the baseline in the subsequent development. In conventional LTE networks, the uplink and downlink schedulers are both deployed in the eNB. Consequently, PDCCH mainly carries resource allocation results to instruct users how to send uplink data on PUSCH or how to decode downlink data on PDSCH, while PUCCH mainly carries downlink CSI feedbacks. As discussed above, in the proposed dual-scheduler configuration, the uplink and downlink scheduling procedures are very similar. As a result, for the proposed dual-scheduler configuration, contents carried by PUCCH and PDCCH tend to be the same. In PDCCH, in addition to the content of existing resource allocation results, the uplink CSI becomes an extra load. While in PUCCH, resource allocation results of uplink scheduling are extra added to help small cells decode uplink data on PUSCH. Since in multi-user scenarios all RBs assigned to one user during a frame share the same MCS, a five bits indication of this MCS is adequate for each user's PDCCH. However, in the proposed resource allocation scheme for the single-user railway scenario (see section III), different types of services with various requirements are distinguished. Hence, more bits of PDCCH/PUCCH will be needed to represent allocated MCSs for each service as shown in Fig. 5. This obviously increases the overhead on PUCCH/PDCCH. Nevertheless, in the single-user railway scenario, the onboard MR-UE is the only accessed user. There exists only one PDCCH/PUCCH and corresponding spectra are all used to transmit this PDCCH/PUCCH instead of being shared among multiple users. Moreover, as discussed above, it is achievable to apply finer resource allocation granularity in the railway scenario, thus further reducing the overhead on PDCCH/PUCCH. Then, the aforementioned problem of excess overhead is not significant. In Fig. 5, bits in S_i block indicate the positions and amounts of resources allocated to service S_i as well as the MCSs used on each resource. Suppose the simplest method bitmap is employed to map the resource allocation results in PDCCH/PUCCH and the amount of total resources is 20. Then, for each service there are 20bits used to indicate positions of allocated resources. For service S_i , bits corresponding to the positions of allocated resources are set to 1 in S_i block. The number of bits set to 1 presents the amount of allocated resources. Besides, in the proposed resource allocation scheme, different resources may be allocated with different MCSs. Thus, additional bits are needed in S_i block to indicate the MCSs used in each allocated resource. As different services may be assigned with different numbers of resources, i.e., the number of bits set to 1 may be different, the amounts of bits used to indicate MCSs are different. This situation is depicted in Fig. 5, where different blocks have different sizes. In addition, an extra area is considered in Fig. 5 to carry the CSI feedback. For simplicity, only PDCCH is described in Fig. 5. It is similar to that for PUCCH. In practice, bitmap is the simplest but most inefficient method to map resource allocation results in PDCCH/PUCCH. In this paper, bitmap is just taken as an example to facilitate the understanding. Many other efficient methods can be used as well. However, this is out of the scope of this paper.

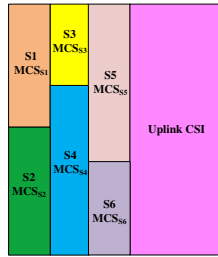


Fig. 5. Contents in PDCCH of the proposed dual-scheduler configuration.

III. THE UPLINK RESOURCE ALLOCATION SCHEME WITH HIGH SPECTRUM EFFICIENCY

Doppler effect in the high-speed movement scenarios is a severe problem to high performance transmissions. Fortunately, in the special railway scenarios, the characteristics of deterministic traveling directions, regular running tracks and repetitive movements of trains along fixed running tracks lead to predictable Doppler shifts, thereby making it easier to track and compensate the Doppler effect under this scenario [17]. Moreover, there have been many research studies focusing on the Doppler spread estimation and compensation for high-speed railway scenarios, such as in [18]. Based on this observation, in this paper we assume that the Doppler effect can be perfectly compensated and has almost no influence on the final performance for both the conventional and proposed uplink resource allocation schemes, which also ensures the fairness when comparing the performance of two schemes in both theoretical analysis and numerical simulations.

Based on the above dual-scheduler configuration, we propose an uplink resource allocation scheme with high spectrum efficiency for most single-user railway scenarios. To facilitate the understanding of the proposed scheme, key variables and their definition used in the following analyses are listed in Table I. Since in practice the value of bandwidth is much smaller than that of central frequency, the whole spectrum displays the same large-scale fading in the view of the single MR-UE. For example, suppose the central frequency is $f_c=5\text{GHz}$ and the bandwidth $B=100\text{MHz}$, then the large-scale path loss difference between the frequency points of $f_c+B/2$ and $f_c-B/2$ is $20\lg((f_c+B/2)/(f_c-B/2))=0.173\text{dB}$, which is negligible. Therefore, as in [15], [16], the proposed uplink resource allocation scheme is based on the small-scale fading. As previously mentioned, for railway scenarios, finer resource allocation granularity is achievable and we call it a chunk. According to [19], the typical time spread of railway scenarios is 200ns and the corresponding coherence bandwidth is $B_c=1\text{MHz}$. It is undoubted that larger resource allocation granularity would decrease the performance to some extent. Fortunately, Zhu and Wang [13] have demonstrated that if $N \cdot \Delta f/B_C < 0.8$, where N is the number of subcarriers in one chunk and Δf is the frequency space between two subcarriers, the performance of chunk-based resource allocation is quite close to that of subcarrier-based resource allocation. Take LTE as the baseline, $\Delta f=15\text{KHz}$ and $N < 53.3$. For simplicity, N is set to 48, that is, 48 subcarriers are tied up in one chunk. With total bandwidth of B , the sum of chunks

is $G = \frac{B}{N \cdot \Delta f}$. In this paper, the expressions of chunk and channel are used interchangeably.

TABLE I
KEY VARIABLES AND THEIR DEFINITIONS.

Variables	Definitions
f_c	Central frequency
B	System bandwidth
B_c	Coherence bandwidth
Δf	Subcarrier frequency space
N	Number of subcarriers in a chunk
G	Number of chunks
M	Number of data streams
g	Subscript of chunk
m	Subscript of data stream
S_m	Data stream m
$PL(d)$	Large-scale path loss
β_g	Average channel gain
K	Rice factor
N_0	Noise power
v_g	MCS efficiency
γ_m	BER constraint
P_g	Transmit power
a_m	Traffic volume
P_{tot}	Total transmit power
T_s	OFDM symbol duration
L	The highest allocated bits

A. Overview of the Proposed Scheme

In this subsection, as shown in Fig. 6, an overall diagram of the proposed uplink resource allocation scheme is presented to facilitate the understanding of this scheme. To improve the average throughput, different types of services with different requirements are distinguished in the proposed uplink resource allocation scheme. In the conventional multi-user scenarios, OFDMA (Orthogonal Frequency Division Multiple Access) means the spectrum multiplexing/sharing among multiple users. While for single-user railway scenarios, the spectrum is multiplexed/shared among multiple services and we call it multi-service OFDMA system. In the multi-service OFDMA system model as shown in Fig. 6, between the transmitter and receiver, different services in one schedule time period are classified into different data streams based on their various BER requirements, where M represents the total number of data streams and γ_m denotes the BER constraint on the data stream S_m . In this system model, receivers estimate uplink CSIs and feed them back to transmitters. Then, based on the requirements of data streams and uplink CSIs, transmitters allocate uplink resources, including chunks, power and bits, for different data streams. Considering practical applications, the available allocated bits should not be equal to arbitrary values, but some predefined discrete values. Therefore, after uplink resource allocations, a discretization procedure for allocated bits is conducted. The information of resource allocation results, including chunk allocation and MCS selection, are fed forward from the transmitter to the receiver. Then, the modulated data in all chunks are forwarded to inverse fast Fourier transform (IFFT) and a cyclic prefix (CP) is added to each OFDM symbol after the parallel-to-serial (P/S) data processing. Afterwards, OFDM data are transmitted to the broadband wireless channel. At the receiver, the CP is first

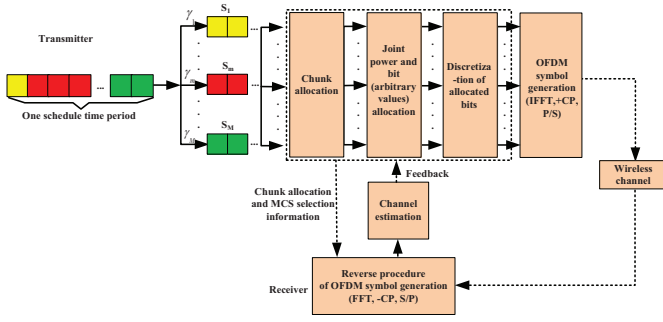


Fig. 6. Overall diagram of the proposed uplink resource allocation scheme.

removed from the received data, and then FFT and S/P are carried out. Finally, the data on allocated chunks are demodulated according to the received resource allocation results provided by the transmitter.

B. Optimization Problem

For an arbitrary chunk g , N subcarriers are tied up, of which the channel gain of the n th subcarrier can be expressed as

$$\beta_{g,n} = PL(d) \cdot |\alpha_{g,n}|^2 \quad (1)$$

where $n = 1, \dots, N$. $PL(d)$ represents the large-scale path loss with propagation distance d . For the small-scale LOS channel $\alpha_{g,n}$, the distributions of its real and imaginary parts obey $N(m_1, \sigma^2)$ and $N(m_2, \sigma^2)$, respectively, where $N(m, \sigma^2)$ stands for Gaussian distribution with mean m and variance σ^2 [20]. We know that $\alpha_{g,n}^2$ follows non-central Chi-square distribution with freedom of 2, that is,

$$f(x) = \frac{1}{2} e^{-(x+\lambda)/2} I_0(\sqrt{\omega x}) \quad (2)$$

where x is the simplified denotation of $\alpha_{g,n}^2$, and the non-centrality parameter ω is calculated as [21]

$$\omega = \frac{m_1^2 + m_2^2}{\sigma^2} = 2K \quad (3)$$

where K is the Rice factor. In practice, the Rice factor K of a wireless channel is known. Then, with (3), we can obtain the non-central parameter ω .

Without loss of generality, the average channel gain of N subcarriers in chunk g is employed as the equivalent channel gain of chunk g , that is,

$$\beta_g = \frac{1}{N} \sum_{n \in N_g} \beta_{g,n} \quad (4)$$

where N_g represents the set of N subcarriers in chunk g .

According to [22], with given MCS and transmit power, BER can be approximated as a close form

$$BER_g \approx 0.2 \exp\left(\frac{-1.6 \cdot P_g \cdot \beta_g \cdot T_s}{N_0 \cdot (2^{v_g} - 1)}\right) \quad (5)$$

where P_g denotes the transmit power per OFDM (Orthogonal Frequency Division Multiplexing) symbol, T_s represents the OFDM symbol duration, N_0 is the power of additive Gaussian white noise, and v_g expresses the MCS efficiency i.e., allocated bits.

If chunk g is allocated to data stream S_m to satisfy

$$BER_{g,m} \leq \gamma_m \quad (6)$$

then we will get

$$v_{g,m} \leq \log_2 \left(1 + \frac{-1.6 \cdot P_{g,m} \cdot \beta_g \cdot T_s}{N_0 \ln(5\gamma_m)} \right) \quad (7)$$

Take the equality case in (7) to maximize the total throughput. Then, we obtain

$$v_{g,m} = \log_2 \left(1 + \frac{-1.6 \cdot P_{g,m} \cdot \beta_g \cdot T_s}{N_0 \ln(5\gamma_m)} \right) = \pi(\gamma_m, P_{g,m}, \beta_g) \quad (8)$$

Suppose the total transmit power of the onboard MR-UE is confined to P_{tot} . Thus, the optimization problem to maximize the total throughput can be modeled as

$$\begin{aligned} \max N \sum_{g=1}^G \sum_{m=1}^M \rho_{m,g} \pi(\gamma_m, P_{g,m}, \beta_g) \\ \text{s.t.}, \begin{cases} C1: \sum_{m=1}^M \rho_{m,g} = 1 \\ C2: \frac{1}{G} \sum_{g=1}^G \rho_{m,g} = a_m \\ C3: N \sum_{g=1}^G \sum_{m=1}^M \rho_{m,g} P_{g,m} \leq P_{tot} \end{cases} \end{aligned} \quad (9)$$

where $\rho_{m,g}$ is defined to indicate whether chunk g is allocated to data stream S_m . If chunk g is allocated to data stream S_m , then $\rho_{m,g} = 1$. Otherwise, $\rho_{m,g} = 0$. Constraint $C1$ ensures that any chunk is allocated to only one data stream. For example, if chunk g is allocated to data stream S_m , then we get $\rho_{m,g} = 1$ and $\rho_{i,g} = 0$ for any $i \neq m$. Constraint $C2$ is employed to guarantee the resource allocation fairness to some extent. For data stream S_m , the number of allocated chunks over total chunks G is equal to a preset resource allocation proportion a_m with $\sum_{m=1}^M a_m = 1$ [23]. With regard to the data stream with higher traffic volume, the resource allocation proportion should be set to a larger value. Therefore, the value of a_m can exactly reflect the traffic volume requirements of data streams. The total transmit power constraint is expressed by $C3$.

In practical wireless communication systems, the available bits for allocation, i.e., $v_{g,m}$, are not equal to arbitrary values but some predefined discrete values, that is,

$$v_{g,m} = \pi(\gamma_m, P_{g,m}, \beta_g) \in \{0, 1, 2, \dots, L\} \quad (10)$$

where L is the highest available bits for allocation.

According to (5), we get

$$P_{g,m} = \frac{\ln(5\gamma_m) \cdot (2^{v_{g,m}} - 1)}{-c\beta_g} = \psi(\gamma_m, v_{g,m}, \beta_g) \quad (11)$$

That is to say, if chunk g is allocated to data stream S_m , the available transmit power for allocation is not arbitrary but discrete as follows

$$P_{g,m} \in \{\psi(\gamma_m, 1, \beta_g), \dots, \psi(\gamma_m, L, \beta_g)\} \quad (12)$$

Consequently, L transmit power matrices $\psi_l^{M \times G}$ with dimensions of $M \times G$ is constructed, where $l = 1, 2, 3, \dots, L$. The

solution to the optimization problem in (9) can be interpreted as the process of searching G transmit power values from these L matrices to maximize the total transmitted bits under the restriction on total transmit power P_{tot} . Then, the optimization problem with discrete available bits and transmit power for allocation can be further modeled as

$$\max N \sum_{g=1}^G \sum_{m=1}^M \sum_{l=1}^L l \cdot \rho_{m,g,l}$$

$$s.t., \begin{cases} C1 : \sum_{m=1}^M \rho_{m,g} = 1 \\ C2 : \frac{1}{G} \sum_{g=1}^G \rho_{m,g} = a_m \\ C3 : N \sum_{g=1}^G \sum_{m=1}^M \sum_{l=1}^L \psi(\gamma_m, l, \beta_g) \cdot \rho_{m,g,l} \leq P_{tot} \end{cases} \quad (13)$$

where

$$\rho_{m,g,l} = \begin{cases} 1, & l \text{ bits are allocated to chunk } g \text{ carrying } S_m \\ 0, & \text{otherwise} \end{cases} \quad (14)$$

Obviously, this optimization problem is a combinational optimization problem. It may be too complicated to employ the method of exhaustion to obtain the optimal solution. Fortunately, based on [24], to reduce complexity, this problem can be divided into two steps to get a suboptimal solution. The first step is chunk allocation, which allocates a chunk to a particular data stream. Chunk allocation is only determined by the channel gain without need of the information on allocated bits and transmit power. The second step is joint power and bits allocation upon the chunk allocation results.

C. Chunk Allocation

To simplify notational expressions, we define $c = \frac{1.6T_s}{N_0}$ and $\Gamma_{g,m} = \frac{2^{v_{g,m}} - 1}{P_{g,m}}$. Then, equation (5) can be simplified as

$$\gamma_m = 0.2 \exp(-c \cdot \Gamma_{g,m} \cdot \beta_g) \quad (15)$$

Physically, larger $\Gamma_{g,m}$ means more efficient transmission of data stream S_m on chunk g . In other words, under the same transmit power, more bits can be transmitted or under the same transmitted bits, lower transmit power is needed. From (15), we can find that with the same $\Gamma_{g,m}$, it is more effective to allocate the chunk with larger channel gain to the data stream with higher BER requirement [15]. The detailed process of chunk allocation is listed as follows. Firstly, sort the G chunks in descending order based on their channel gains, i.e., $\beta_{(1)} > \beta_{(2)} > \dots > \beta_{(G)}$. Then, sort the data streams in ascending order based on their BER requirements, i.e., $\gamma_{(S1)} < \gamma_{(S2)} < \dots < \gamma_{(SM)}$. According to the constraint C2 in (9), the number of chunks that should be allocated to S_m is $a_m G$. Consequently, chunks with the largest channel gains $\beta_{(1)}, \dots, \beta_{(a_{(S1)}G)}$ are allocated to the data stream with the highest BER requirement $\gamma_{(S1)}$. Then, $\beta_{(a_{(S1)}G+1)}, \dots, \beta_{(a_{(S1)}G+a_{(S2)}G)}$ are allocated to the data stream with BER requirement $\gamma_{(S2)}$. The rest can be done in the same manner. For a chunk, it can only be allocated to a data stream. While for a data stream, its data may be distributed to multiple chunks.

D. Joint Power and Bit Allocation

Based on the above chunk allocation, the optimization problem of joint power and bit allocation can be expressed as

$$\max N \sum_{g=1}^G \sum_{l=1}^L l \cdot \rho_{m,g,l}, \quad m = 1, \dots, M$$

$$s.t., N \sum_{g=1}^G \sum_{l=1}^L \psi(\gamma_m, l, \beta_g) \cdot \rho_{m,g,l} \leq P_{tot} \quad (16)$$

It should be noted that after the chunk allocation M data streams are distributed on G chunks, i.e., every chunk is allocated with a dedicated data stream. The transmit power allocated to a chunk is to guarantee the BER demand of the data stream on this chunk, as well as to maximize the total throughput. Hence, as in (16), the constraint is directly determined by the total transmit power of all chunks now. The optimization problem in (16) may be a complicated combinational optimization problem. To find an approximate solution, the predefined discrete values for the constraint corresponding to the available allocated bits are relaxed to arbitrary values. Thus, the optimization model in (16) can be rewritten as

$$\max N \sum_{g=1}^G \pi(\gamma_{mg}, P_{g,mg}, \beta_g), \quad m = 1, \dots, M$$

$$s.t., N \sum_{g=1}^G P_{g,mg} \leq P_{tot} \quad (17)$$

where the subscript mg means that chunk g has been allocated to S_m . Take the equality constraint in (17), this problem can be solved by Lagrangian method as given in Appendix A. Then, the expression of transmit power allocated to chunk g can be obtained as

$$P_{g,mg} = \frac{P_{tot}}{NG} + \frac{1}{c} \left(\frac{\ln(5\gamma_{mg})}{\beta_g} - \frac{1}{G} \sum_{i=1}^G \frac{\ln(5\gamma_{mi})}{\beta_i} \right) \quad (18)$$

To simplify the analysis, variable $\mu_{i,mi}$ called channel carrying capability, is defined as

$$\mu_{i,mi} = \frac{\ln(5\gamma_{mi})}{\beta_i} \quad (19)$$

In practice, the BER constraint γ_{mi} is usually smaller than 10^{-2} . Therefore, $\mu_{i,mi} < 0$. For arbitrary chunk i with particular data stream S_m distributed on it, the larger the $|\mu_{i,mi}|$, the higher the channel carrying capacity of chunk i . Based on the definition of (19), (18) can be rewritten as

$$P_{g,mg} = \frac{P_{tot}}{NG} + \frac{1}{c} \left(\mu_{g,mg} - \frac{1}{G} \sum_{i=1}^G \mu_{i,mi} \right) \quad (20)$$

From (18), we can find that the allocated transmit power is based on the average value $\frac{P_{tot}}{NG}$. Then, for a given chunk g , its exact allocated transmit power is further adjusted according to the difference between its channel carrying capacity and the average channel carrying capacity of all chunks. For the chunk with higher channel carrying capacity, the value of $\mu_{g,mg} - \frac{1}{G} \sum_{i=1}^G \mu_{i,mi}$ is smaller than 0. That is, the needed transmit power is lower than $\frac{P_{tot}}{NG}$, which in turn proves that this chunk is really of high channel carrying capacity. While for the chunk

with lower channel carrying capacity, the value of $\mu_{g,mg} - \frac{1}{G} \sum_{i=1}^G \mu_{i,mi}$ may be even larger than 0, that is, the needed transmit power is much larger.

Consequently, the amount of allocated bits in chunk g for data stream S_m is

$$R_{g,mg} = \log_2 \left(1 - \frac{cP_{g,mg}\beta_g}{\ln(5\gamma_{mg})} \right) = \log_2 \left(\frac{\beta_g}{\ln(5\gamma_{mg})} \cdot \left(\frac{-cP_{tot}}{NG} + \frac{1}{G} \sum_{i=1}^G \frac{\ln(5\gamma_{mi})}{\beta_i} \right) \right) \quad (21)$$

E. Bit Allocation

Up to now, with relaxed constraint of available bits for allocation, the obtained $R_{g,mg}$ is equal to arbitrary values. However, in practical wireless communication systems, the available bits for allocation are predefined, i.e., $R_{g,mg} \in \{0, 1, 2, \dots, L\}$. Based on this, to discretize $R_{g,mg}$, variables $R^-_{g,mg}$ and $R^+_{g,mg}$ are defined as follows

$$R^-_{g,mg} = \begin{cases} 0, & R_{g,mg} < 1 \\ 1, & 1 \leq R_{g,mg} < 2 \\ \vdots \\ L-1, & L-1 \leq R_{g,mg} < L \\ L, & R_{g,mg} \geq L \end{cases} \quad (22)$$

$$R^+_{g,mg} = \begin{cases} R^-_{g,mg} + 1, & R^-_{g,mg} \leq L-1 \\ L, & R^-_{g,mg} = L \end{cases} \quad (23)$$

From (22), $R^-_{g,mg}$ is equivalently equal to the rounding down value of $R_{g,mg}$, which means the total transmit power does not reach the constraint P_{tot} . However, with some residual power, the achieved throughput is not the highest. While it is opposite for the definition of $R^+_{g,mg}$, under which the highest throughput can be achieved. Nevertheless, the total transmit power may exceed the constraint P_{tot} . Thus, the discretization process of $R_{g,mg}$ is to make reasonable choices between $R^-_{g,mg}$ and $R^+_{g,mg}$ to maximize the total throughput with just the right exhaustion of total transmit power P_{tot} . For $R^-_{g,mg}$ and $R^+_{g,mg}$, the corresponding transmit power values are

$$\begin{aligned} P^-_{g,mg} &= \psi(\gamma_m, R^-_{g,mg}, \beta_g) \\ P^+_{g,mg} &= \psi(\gamma_m, R^+_{g,mg}, \beta_g) \end{aligned} \quad (24)$$

The additional power needed for the selection of $R^+_{g,mg}$ is

$$\Delta P_{g,mg} = P^+_{g,mg} - P^-_{g,mg} \quad (25)$$

The detailed discretization procedure is depicted in Fig. 7, where $R^*_{g,mg}$ and $P^*_{g,mg}$ denote the optimal allocated bits and the corresponding transmit power, respectively. During the discretization procedure, whether a chunk is added by one bit depends on whether the additional power needed by the chunk for the one-bit-increase per symbol per subcarrier is the smallest among all other chunks. Afterwards, no more bits are allocated to this chunk and another one bit per symbol per subcarrier is added to another chunk which requires the smallest additional power among remaining chunks. This one-bit-increase per symbol per subcarrier algorithm is repeated in the discretization procedure until the total power constraint

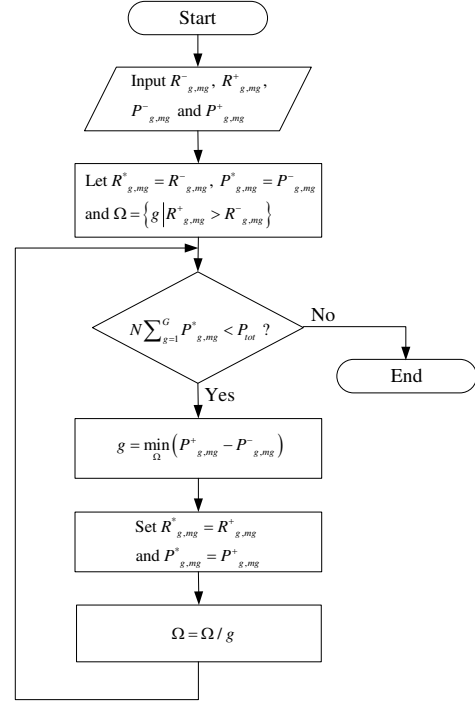


Fig. 7. The discretization procedure.

is satisfied. Actually, the criterion of the discretization procedure is that the total one-bit increase ensures the minimum corresponding to total additional power, so as to maximize the utilization of transmit power.

Consequently, the achieved total throughput can be expressed as

$$R_{\max} = N \sum_{g=1}^G R^*_{g,mg} \quad (26)$$

Through the above three steps, including chunk allocation, joint power and bit allocation and discretization of allocated bits, we obtain the suboptimal solution to the complicated combinational optimization problem of (13). Although relaxations are applied in the solution algorithms, the purpose of every step is to maximize the throughput rather than to find an approximate solution. Therefore, the proposed resource allocation scheme can still highly improve the transmission performance.

IV. NUMERICAL RESULTS

In this section, we carry out performance evaluation on our proposed scheme. Simulation parameter values are listed in Table II. In order to investigate the influence of data stream requirement differences on performance, here two data streams are taken into account. Based on [25], the correlation coefficient of two subcarriers in one chunk can be calculated via

$$\rho_{n_1, n_2} = \frac{1}{\sqrt{1 + \left(\frac{|f_{n_1} - f_{n_2}|}{B_c} \right)^2}} \quad (27)$$

where f_{n_1} and f_{n_2} are the central frequencies of subcarrier n_1 and n_2 , respectively.

TABLE II
SIMULATION PARAMETERS.

Parameters	Values
Number of subcarriers in a chunk N	48
Number of chunks G	20
Coherence bandwidth B_c	1MHz
Rice factor K	10dB
Number of data streams M	2
Total transmit power P_{tot}	20W
The highest allocated bits L	6
Noise power N_0	-174dBm/Hz
OFDM symbol duration T_s	71.4us

A. Performance Comparisons under Different Path Loss

As mentioned before, the value of a_m can exactly reflect the traffic volume requirement on data stream S_m . Thus, we directly use a_m as the equivalent traffic volume requirement. Firstly, by taking the BER and traffic volume requirements on two data streams as constant values, the investigation of average throughput in different large-scale path loss situations is conducted. In this paper, we primarily consider the small-scale fading in the proposed uplink resource allocation scheme (simplified as “proposed scheme” for following analysis). However, large-scale path loss determines the overall channel quality and corresponding investigation can provide the overall performance trend. For data stream S_1 , $\gamma_1 = 10^{-6}$ and $a_1=0.7$. For data stream S_2 , $\gamma_2 = 10^{-2}$ and $a_2=0.3$. In the conventional eNB-centralized uplink resource allocation scheme (simplified as “conventional scheme” for following analysis), the stricter BER constraint of the two BER requirements is chosen as the BER constraint for both data streams [15]. Thus, the equivalent BER constraint here is 10^{-6} . In the conventional scheme, all resources allocated to one user adopt the same MCS, indicating that the total transmit power is equally distributed over all resources. Hence, for each subcarrier, the allocated transmit power is $P_{tot}/(GN)$. By substituting the transmit power and BER constraint into (8), the corresponding transmitted bits per subcarrier are obtained.

For clarity, the average throughput is used as the performance indicator, which is defined as the carrying bits of every OFDM symbol, i.e., $R_{ave} = \frac{R_{max}}{NG}$ with unit of bits/ T_s /subcarrier. The performance comparison of the conventional and proposed schemes with and without discretization in different large-scale path loss situations is shown in Fig. 8. Obviously, no matter with or without discretization, the average throughput of the proposed scheme performs better than that of the conventional scheme. Compared with the case without discretization, the performance improvement of the proposed scheme is more prominent for the case with discretization. For the case with discretization, when the path loss is low, such as in (70-80dB), both schemes reach the highest average throughput at 6bits/ T_s /subcarrier. With decrease in the channel quality, the average throughput of two schemes decreases. Nevertheless, with consideration of the requirement differences between two data streams, the proposed scheme always outperforms the conventional scheme. While for the case without discretization in which there is no limitation on capacity (the highest 6bits/ T_s /subcarrier), the average throughput of both schemes almost linearly decreases

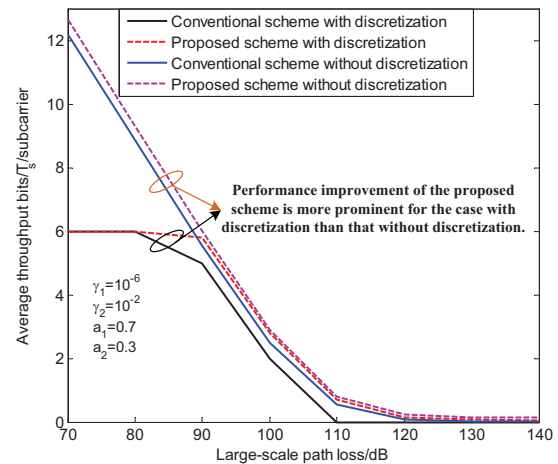


Fig. 8. Average throughput in different large-scale path loss situations.

when path loss varies in the range of (70-100dB). When the path loss gets much larger, the average throughput of two schemes decreases more slowly. It should be noted that with the highest 6bits/ T_s /subcarrier limitation, the average throughput for the case with discretization cannot increase as path loss decreases from 80dB to 70dB, but keeps at the highest level. Correspondingly, in this situation, the total consumed transmit power is less than P_{tot} , i.e., some transmit power is saved. While without that limitation, to maximize the average throughput, the total transmit power can be used up for the case without discretization. Hence, as shown in Fig. 8, the average throughput for the case without discretization almost increases linearly as path loss decreases from 80dB to 70dB. However, this does not conform to practical wireless communication systems where the available bits for allocation are not equal to arbitrary values but some predefined discrete values with a limited maximum value. Also because the allocated bits are continuous without discretization, the performance curves for the case without discretization are smoother than that with discretization. Moreover, from Fig. 8 we can see that although the average throughput of the proposed scheme with discretization is a little bit lower than that of the proposed scheme without discretization, the average throughput of the conventional scheme with discretization is much smaller than that of the conventional scheme without discretization.

B. Performance Comparisons under Different BER Constraints

Next, we study the influence of BER constraint difference between two data streams on performance. The BER constraint of data stream S_1 , taken from the stricter one, is fixed to 10^{-6} . The BER constraint of data stream S_2 varies from 10^{-6} to 10^{-1} . The numerical results are depicted in Fig. 9(a) and Fig. 9(b), respectively, where the large-scale path loss is set to 90dB or 110dB. At the point $\gamma_2 = 10^{-6}$, two data streams possess the same BER constraint, which is equivalent to that only data stream S_1 exists. Then, the effect of BER constraint and traffic volume differences between two data streams on the average throughput vanishes at this point. Nevertheless,

in the conventional scheme, all channels adopt the same MCS and transmit power without any adjustment to small-scale fading differences among channels, which will cause performance degradation. Conversely, the small-scale fading differences among chunks are taken into account during the MCS and transmit power allocation in the proposed scheme. Therefore, at the point $\gamma_2 = 10^{-6}$, the proposed scheme should outperform the conventional scheme. However, for the case without discretization, in Fig. 9(a) where the overall channel is of high quality, the small-scale fading differences among chunks are submerged and two schemes reach the same performance at this point. While in Fig. 9(b) where the channel quality is much poorer, the performance differences between two schemes become obvious. While for the case with discretization, as shown in Fig. 9(a), even under good channels, the performance difference between two schemes is also prominent. That implies that the discretization process highlights the effect of small-scale fading differences on performance, leading to more remarkable performance improvements of the proposed scheme. Moreover, from both Fig. 9(a) and Fig. 9(b), we can see that since in the conventional scheme with and without discretization the strictest BER constraint is always selected as the reference for resource allocation, the changes of S_2 's BER constraint do not have any effect on the performance of the conventional scheme, which is shown in both figures that the average throughput of the conventional scheme stays at a constant level. While in the proposed scheme with and without discretization, the BER requirement difference between two data streams is distinguishable. Hence, as γ_2 increases, i.e., the BER constraint difference between two data streams enlarges, the performance of the proposed scheme continuously rises. Furthermore, for the proposed scheme, the larger the BER constraint difference, the higher the performance improvement. That is, for the curves of the proposed scheme with and without discretization in both figures, the slope increases with the increasing of γ_2 . Nevertheless, in Fig. 9(a), under the limitation that the highest allocated bits are 6bits/ T_s /subcarrier, with γ_2 increasing, the average throughput of the proposed scheme with discretization maintains the highest level eventually. While without that limitation, the obtained average throughput of the proposed scheme without discretization continues to grow.

C. Performance Comparisons under Different Traffic Volumes

Finally, we investigate the effect of traffic volume difference between two data streams on performance. The BER constraints of two data streams are fixed to $\gamma_1 = 10^{-6}$ and $\gamma_2 = 10^{-2}$, respectively. The traffic volume difference can be expressed as $a_2 - a_1 = 2a_2 - 1$. The numerical results are shown in Fig. 10(a) and Fig. 10(b), where the large-scale path loss is set to 90dB or 110dB. At the point $2a_2 - 1 = -1$, the traffic volume of data stream S_2 is 0, that is, only data stream S_1 is present. In Fig. 10(b), for the case without discretization, the same reason that in the conventional scheme all channels adopt the same MCS and transmit power without any adjustment to small-scale fading differences among channels, results in the performance degradation. On the contrary, for

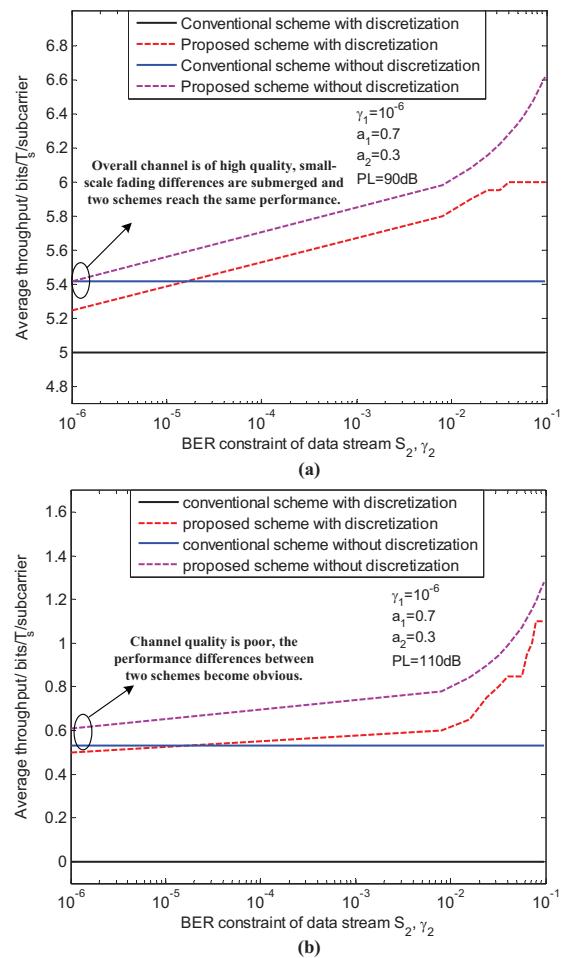


Fig. 9. Average throughput versus BER constraint difference.

the proposed scheme, the small-scale fading differences among chunks are taken into account during the MCS and transmit power allocation. Thus, at that point, the proposed scheme still outperforms the conventional scheme. While in Fig. 10(a) where the overall channel is of high quality, the small-scale fading differences among chunks are submerged without the discretization process. Hence, the above performance differences between two schemes are not obvious. While for the case with discretization, no matter whether the overall channel quality is good or bad, the performance improvements of the proposed scheme are always prominent as shown in both Fig. 10(a) and Fig. 10(b). Moreover, in the conventional scheme with and without discretization, two data streams are regarded as one data stream. Therefore, in both figures, the average throughput maintains a constant value all the time. While in the proposed scheme with and without discretization, two data streams with different BER constraints are distinguishable, which introduces performance improvements. Based on the setting, the BER constraint of data stream S_2 is much less strict than that of S_1 . With the same transmit power, lower BER requirement means more achievable bits to transmit. Therefore, as more chunks are allocated to data stream S_2 , higher performance is achieved in the proposed scheme as shown in both figures. Nevertheless, in Fig. 10(a) where the

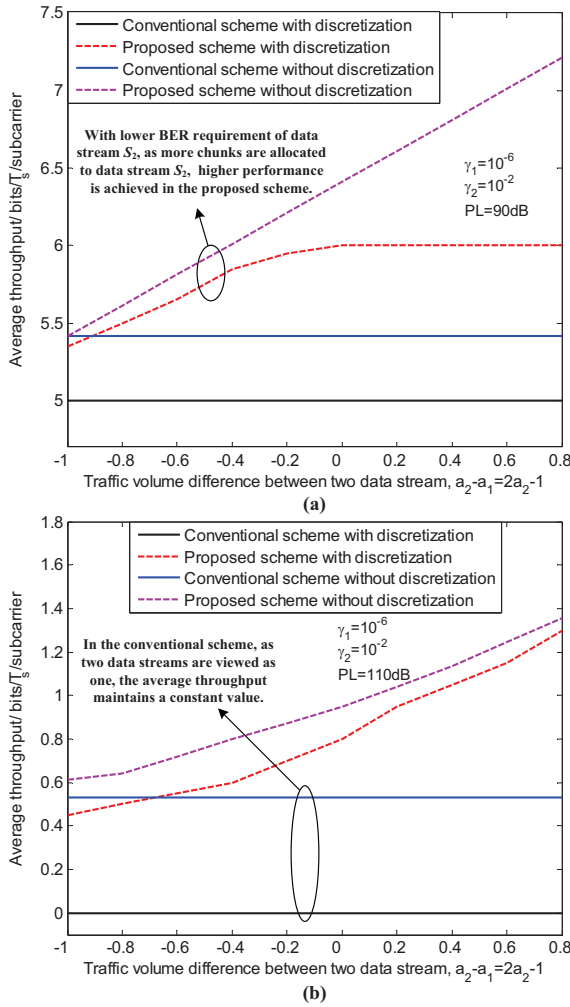


Fig. 10. Average throughput versus traffic volume difference.

path loss is low, with the highest $6\text{bits}/T_s/\text{subcarrier}$ limitation, as $2a_2 - 1$ increases, the average throughput of the proposed scheme with discretization maintains the highest level eventually. While without that limitation, the average throughput of the proposed scheme without discretization still increases with increasing $2a_2 - 1$.

V. CONCLUSION

To meet the enormous capacity demands of train passengers' services in railway scenarios, we proposed the C/U-plane decoupled railway network, in which higher frequency bands with broader bandwidth are assigned to small cells to transmit passengers' data (U-plane) while utilizing lower frequency bands to handle control signaling (C-plane). Then how to efficiently utilize these spectra becomes an urgent problem. Except when trains move in opposite directions or cross train stops, for a given wayside eNB in the C/U-plane decoupled railway wireless network, the onboard MR-UE is mostly the only accessed user with the whole spectrum allocated. Based on this observation, an additional uplink scheduler is configured in the MR-UE in the proposed dual-scheduler configuration, which enables the MR-UE to self-manage the

usage of uplink resources. In this way, in contrast with the conventional eNB-centralized scheduler configuration, the complicated procedure of uplink grant request is avoided and significant uplink scheduling time is saved. Furthermore, based on the characteristics of the C/U-plane decoupled architecture, eNB schedulers are configured in small cells. As the macro cell is the first one aware of any other random access request, the uplink scheduler switcher is added in the macro cell. If the onboard MR-UE is the only accessed user, the uplink scheduler in the MR-UE is activated by the uplink scheduler switcher. Otherwise, if any other random access request is accepted, the uplink scheduler in small cells is selected.

Based on the above dual-scheduler configuration, we develop an uplink resource allocation scheme with high spectrum efficiency. Numerical results have demonstrated that the proposed uplink resource allocation scheme can greatly improve the average throughput compared with the conventional scheme. In the proposed scheme, we assumed that trains can obtain perfect uplink CSIs to instruct resource allocations. However, this assumption may be violated in practical railway wireless communication systems. On one hand, due to the feedback delay especially in high-speed railway scenarios, CSIs may degrade the effectiveness when they arrive at the transmitters. On the other hand, considering the feedback overhead, codebook based CSI feedback method has generally been used in practical wireless communication systems. Consequently, channel estimation errors and quantization errors can also make the above assumption invalid. Therefore, in our future research, the effect of imperfect channel information on the proposed scheme needs further investigation.

APPENDIX A

Using Lagrangian method to solve (17), let

$$LM = N \sum_{g=1}^G \pi(\gamma_{mg}, P_{g,mg}, \beta_g) + \lambda \left(N \sum_{g=1}^G P_{g,mg} - P_{tot} \right)$$

where λ is the Lagrangian multiplier for the constraint in (17). The solution can be derived by differentiating LM with respect to all $P_{g,mg}$ and setting each derivative to zero. Then, we can obtain a set of equations with G components

$$\begin{cases} \frac{\partial LM}{\partial P_{1,m1}} = N \left(\frac{\partial \pi(\gamma_{m1}, P_{1,m1}, \beta_1)}{\partial P_{1,m1}} + \lambda \right) = 0 \\ \vdots \\ \frac{\partial LM}{\partial P_{G,mG}} = N \left(\frac{\partial \pi(\gamma_{mG}, P_{G,mG}, \beta_G)}{\partial P_{G,mG}} + \lambda \right) = 0 \end{cases}$$

By substituting (8) into (19) we can get

$$\begin{cases} \frac{-c\beta_1}{\ln 2 \cdot (\ln(5\gamma_{m1}) - cP_{1,m1}\beta_1)} + \lambda = 0 \\ \vdots \\ \frac{-c\beta_G}{\ln 2 \cdot (\ln(5\gamma_{mG}) - cP_{G,mG}\beta_G)} + \lambda = 0 \end{cases}$$

Consequently,

$$\frac{\beta_1}{\ln(5\gamma_{m1}) - cP_{1,m1}\beta_1} = \dots = \frac{\beta_G}{\ln(5\gamma_{mG}) - cP_{G,mG}\beta_G}$$

The transmit power values of all chunks can be expressed as the transmit power of arbitrary chunk g , $P_{g,mg}$, that is,

$$\begin{cases} P_{1,m1} = \frac{\ln(5\gamma_{m1})/\beta_1 - \ln(5\gamma_{mg})/\beta_g + cP_{g,mg}}{c} \\ \vdots \\ P_{g,mg} = \frac{\ln(5\gamma_{mg})/\beta_g - \ln(5\gamma_{mg})/\beta_g + cP_{g,mg}}{c} \\ \vdots \\ P_{G,mG} = \frac{\ln(5\gamma_{mG})/\beta_G - \ln(5\gamma_{mg})/\beta_g + cP_{g,mg}}{c} \end{cases}$$

By combining with the total transmit power constraint $N \sum_{i=1}^G P_{i,mi} = P_{tot}$ in (17), the expression of transmit power allocated to chunk g can be derived as (18).

ACKNOWLEDGMENT

The work of authors was supported partially by the 973 Program under Grant 2012CB316100, NSFC under Grants 61471303, the Program for Development of Science and Technology of China Railway Corporation under Grant 2013X016-A, and EP7-PEOPLE-2013-IRSES Project under Grant 612652. The work of Y. Fang was partially supported by the US National Science Foundation under grant CNS-1343356.

REFERENCES

[1] W. Luo, R. Zhang, and X. Fang, "A CoMP soft handover scheme for LTE systems in high speed railway," *EURASIP J. Wireless Commun. Netw.*, 2012, 1:196 (doi:10.1186/1687-1499-2012-196).

[2] B. Dusza, C. Ide, P.-B. Bok, and C. Wietfeld, "Optimized cross-layer protocol choices for LTE in high-speed vehicular environments," in *Proceeding of International Wireless Communications and Mobile Computing Conference (IWCMC)*, Sardinia, Italy, Jul. 2013, pp. 1046–1051.

[3] T. Nakamura, S. Nagata, A. Benjebbour, Y. Kishiyama, T. Hai, S. Xiaodong, Y. Ning, and L. Nan, "Trends in small cell enhancements in LTE advanced," *IEEE Commun. Mag.*, vol. 51, no. 2, pp. 98–105, Feb. 2013.

[4] B. Bjerke, "LTE-advanced and the evolution of LTE deployments," *IEEE Wireless Commun. Mag.*, vol. 18, no. 5, pp. 4–5, Oct. 2011.

[5] H. ISHII, Y. Kishiyama, and H. Takahashi, "A novel architecture for LTE-B :C-plane/U-plane split and phantom cell concept," in *proceeding of IEEE Globecom Workshops Workshop on Emerging Technologies for LTE-Advanced and Beyond-4G*, Anaheim, USA, Dec. 2012, pp. 624–630.

[6] X. Xu, G. He, S. Zhang, Y. Chen, and S. Xu, "On functionality separation for green mobile networks: concept study over LTE," *IEEE Commun. Mag.*, vol. 51, no. 5, pp. 82–90, May 2013.

[7] L. Yan, X. Fang, and Y. Fang, "Control and data signaling decoupled architecture for railway wireless networks," *IEEE Wireless Commun.*, vol. 22, no. 1, pp. 103–111, Feb. 2015.

[8] L. Yan and X. Fang, "Reliability evaluation of 5G C/U-plane decoupled architecture for high-speed railway," *EURASIP J. Wireless Commun. Netw.*, 2014, 2014:127 (doi:10.1186/1687-1499-2014-127).

[9] X. Zhu, S. Chen, H. Hu, X. Su, and Y. Shi, "TDD-based mobile communication solutions for high-speed railway scenarios," *IEEE Wireless Commun.*, vol. 20, no. 6, pp. 22–29, Dec. 2013.

[10] E. Dahlman, S. Parkvall, and J. Sköld, *LTE/LTE-Advanced for Mobile Broadband*. Elsevier Ltd, 2011.

[11] L. Electronics, "R1-060051:link adaptation in e-utra downlink," 3GPP TSG RAN WG1 LTE Ad Hoc, Helsinki, Finland, 2006.

[12] V. Papoutsis and S. Kotsopoulos, "Chunk-based resource allocation in multicast OFDMA systems with average BER constraint," *IEEE Commun. Lett.*, vol. 15, no. 5, pp. 551–553, May 2011.

[13] H. Zhu and J. Wang, "Chunk-based resource allocation in OFDMA systems-Part I: chunk allocation," *IEEE Trans. Commun.*, vol. 57, no. 9, pp. 2734–2744, Sept. 2009.

[14] —, "Chunk-based resource allocation in OFDMA systems-Part II: Joint chunk, power and bit allocation," *IEEE Trans. Commun.*, vol. 60, no. 2, pp. 499–509, Feb. 2012.

[15] H. Zhu, "Radio resource allocation for OFDMA systems in high speed environments," *IEEE J. Select. Areas Commun.*, vol. 30, no. 4, pp. 748–759, May 2012.

[16] P. Wang and P.-Y. Kam, "Feedback power control with bit error outage probability qos measure on the rayleigh fading channel," *IEEE Trans. Commun.*, vol. 61, no. 4, pp. 1621–1631, Apr. 2013.

[17] Y. Zhao, C. Yin, and J. Li, "Learning- and optimization-based channel estimation for cognitive high-speed rail broadband wireless communications," in *Proceeding of International Symposium on Communications and Information Technologies (ISCIT)*, Gold Coast, QLD, Australia, Oct. 2012, pp. 562–567.

[18] Q. Du, G. Wu, Q. Yu, and S. Li, "ICI mitigation by Doppler frequency shift estimation and pre-compensation in LTE-R systems," in *Proceeding of IEEE International Conference on Communications in China (ICCC)*, Beijing, China, Aug. 2012, pp. 469–474.

[19] L. Liu, C. Tao, J. Qiu, H. Chen, L. Yu, W. Dong, and Y. Yuan, "Position-based modeling for wireless channel on high-speed railway under a viaduct at 2.35 GHz," *IEEE J. Select. Areas Commun.*, vol. 30, no. 4, pp. 834–845, May 2012.

[20] J. Proakis, *Digital Communications*. Fourth Edition, McGraw Hill, 2000.

[21] Wikipedia. [online]. Available: http://en.wikipedia.org/wiki/Noncentral_chi-square_distribution.

[22] S. T. Chung and A. Goldsmith, "Degrees of freedom in adaptive modulation: a unified view," *IEEE Trans. Commun.*, vol. 49, no. 9, pp. 1561–1571, Sept. 2001.

[23] Y. Qian, C. Ren, S. Tang, and M. Chen, "Multi-service QoS guaranteed based downlink cross-layer resource block allocation algorithm in LTE systems," in *Proceeding of IEEE International Conference on Wireless Communications & Signal Processing (WCSP)*, Nanjing, China, Nov. 2009, pp. 1–4.

[24] C. Y. Wong, R. Cheng, K. Lataief, and R. Murch, "Multiuser OFDM with adaptive subcarrier, bit, and power allocation," *IEEE J. Sel. Areas Commun.*, vol. 17, no. 10, pp. 1747–1758, Oct. 1999.

[25] Y. Zhou and J. Wang, "Downlink transmission of broadband OFCDM systems-part iv: soft decision," *IEEE J. Sel. Areas Commun.*, vol. 24, no. 6, pp. 1208–1220, Jun. 2006.

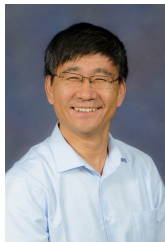


Li Yan received a BE degree in communication engineering from Southwest Jiaotong University, Chengdu, China, where she is currently pursuing her Ph.D. degree with the Key Laboratory of Information Coding and Transmission, School of Information Science and Technology. Her research interests include mobility management, network architecture, and reliable wireless communication for high-speed railways.



Xuming Fang received a BE degree in electrical engineering in 1984, an ME degree in computer engineering in 1989, and a Ph.D. degree in communication engineering in 1999 all from Southwest Jiaotong University, Chengdu, China. He was a Faculty Member with the Department of Electrical Engineering, Tongji University, Shanghai, China, in September 1984. He then joined the School of Information Science and Technology, Southwest Jiaotong University, Chengdu, where he has been a Professor since 2001, and the Chair of the Department of

Communication Engineering since 2006. He held visiting positions with the Institute of Railway Technology, Technical University at Berlin, Berlin, Germany, in 1998 and 1999, and with the Center for Advanced Telecommunication Systems and Services, University of Texas at Dallas, Richardson, in 2000 and 2001. He has published around 200 papers in technical journals and conference and authored/coauthored five books. His research interests include wireless broadband access control, radio resource management, multihop relay networks, and broadband wireless access for high speed railway. Dr. Fang is the Chair of IEEE Vehicular Technology Society of Chengdu Chapter.



Yuguang Fang (F'08) received an MS degree from Qufu Normal University, Shandong, China in 1987, a Ph.D degree from Case Western Reserve University in 1994, and a Ph.D. degree from Boston University in 1997. He joined the Department of Electrical and Computer Engineering at University of Florida in 2000 and has been a full professor since 2005. He held a University of Florida Research Foundation (UFRF) Professorship (2006-2009), a Changjiang Scholar Chair Professorship with Xidian University, China (2008-2011), and a Guest Chair Professorship

with Tsinghua University, China, from (2009-2012).

Dr. Fang received the US National Science Foundation Career Award in 2001 and the Office of Naval Research Young Investigator Award in 2002, 2015 IEEE Communications Society CISTC Technical Recognition Award, 2014 IEEE Communications Society WTC Recognition Award, and the Best Paper Award from IEEE ICNP (2006). He has also received a 2010-2011 UF Doctoral Dissertation Advisor/Mentoring Award, 2011 Florida Blue Key/UF Homecoming Distinguished Faculty Award, and the 2009 UF College of Engineering Faculty Mentoring Award. He is the Editor-in-Chief of IEEE Transactions on Vehicular Technology, was the Editor-in-Chief of IEEE Wireless Communications (2009-2012), and serves/served on several editorial boards of journals including IEEE Transactions on Mobile Computing (2003-2008, 2011-present), IEEE Transactions on Communications (2000-2011), and IEEE Transactions on Wireless Communications (2002-2009). He has been actively participating in conference organization such as serving as the Technical Program Co-Chair for IEEE INFOCOM'2014 and the Technical Program Vice-Chair for IEEE INFOCOM'2005. He is a fellow of the IEEE and a fellow of The American Association for the Advancement of Science (AAAS).



Xiangle Cheng received a BE degree in communication engineering in 2012, and an MS degree in information and communication system in 2015 both from Southwest Jiaotong University, Chengdu, China. He is now a Ph.D. student in the Department of Mathematics and Computer Science, College of Engineering, Mathematics and Physical Sciences, University of Exeter. His research interests include multiple antennas and system architecture for high-speed railways.